Nonlinear Dyn (2022) 110:2225–2245
https://doi.org/10.1007/s11071-022-07752-5

ORIGINAL PAPER

Stochastic response analysis and robust optimization of nonlinear turbofan engine system

Dengji Zhou · Dawen Huang

Received: 29 May 2022 / Accepted: 1 August 2022 / Published online: 13 August 2022

Abstract The quantitative analysis of the uncertainty influence on thermodynamic parameters and performance parameters is usually difficult to achieve due to the strong nonlinear working process in engine systems. It is very important to fully consider the uncertainty influences in the performance design for tapping the working potential. Therefore, this paper establishes a stochastic dynamic model based on the nonlinear characteristics of engine systems, analyzes the time-varying influence law of uncertainty on the responses of thermodynamic parameters and ascertains the stochastic response distribution features of thermodynamic parameters and performance parameters. Based on the quantitative analysis results, an optimization method considering stochastic responses is further established to design the performance parameters of engine systems and compared with the traditional mechanism model and Monte Carlo simulation. The results indicate that the thermodynamic parameters and performance parameters all show the normal distributions, and the fuel system actuation uncertainty has a greater impact on the stochastic responses. The robust optimization method significantly reduces the uncertainty influence and improves the thermodynamics performance with an 84.4% probability. Moreover, it reduces the computational cost by more than half. This work provides an effective method for the quantitative analysis of the uncertainty influence in engine systems and provides a useful reference for the robust performance design of new type engine.

Keywords Nonlinear engine system · Stochastic dynamics · Actuator uncertainty · Stochastic response analysis · Perfromance optimization design

1 Introduction

The performance optimization is a key step in the upgrading, retrofitting and development of turbofan engines, which directly faces the engine performance requirements and mission scenarios [1, 2]. High performance is a common pursuit in the turbofan engine design. Once the geometric structure and cycle parameters are determined, its performance is difficult to be further improved [3]. The complex structures, wide operating regions and strong nonlinear features bring more uncertainties to the engine working performance [4–6]. To improve the reliability and performance robustness, it is necessary to focus on the influences of uncertainties on the engine performance and further consider them in the performance design stage [7, 8].

D. Zhou (✉) · D. Huang
The Key Laboratory of Power Machinery and Engineering of Education Ministry, Shanghai Jiao Tong University, Shanghai 200240, People's Republic of China
e-mail: ZhouDJ@sjtu.edu.cn

Uncertainties in the turbofan engine usually include cognitive uncertainty and stochastic uncertainty. Cognitive uncertainty is formed by the lack of knowledge of the component performance, unmodeled or inaccurate component modeling, for example the lack of accurate performance characteristics of variable geometry component and the lack of understanding of the impact of actuator nonlinear characteristics [9, 10], which will affect the engine performance analysis and design. Cognitive uncertainty can be reduced through refined component modeling [11], a large number of simulations and experiments, hardware-in-the-loop experiments [12, 13], extensive applications and knowledge accumulation [14]. Stochastic uncertainties are inevitable in engine systems, such as tolerances introduced in the manufacturing process and errors caused by the assembly process, etc.. The accumulated uncertainty will lead to the performance deviation through the transmission of the nonlinear operation process [15–17]. The component degradation caused by the high-temperature and high-pressure operating environment also leads to strong stochastic uncertainty [18, 19]. In addition, the wear of actuators during long-term operation is also an important uncertainty source [20]. At present, there are many studies on the robust optimization considering component performance uncertainty. Zhang et al. studied the performance robust design method of variable cycle engine under component performance uncertainty [21]. Cao et al. simulated the influence of component performance uncertainty on the overall performance [22]. However, there are few studies on the actuator uncertainty in the performance robust optimization. The actuators, such as fuel valve, variable stator vane, nozzle area, etc., directly determine the energy working performance. The actuator uncertainty will cause the control commands not to act on the engine system accurately and timely, which may lead to a large deviation between the system performance and the required performance [23, 24]. Nonlinear operation process will aggravate this phenomenon. Therefore, the actuator uncertainties should be paid more attentions in the performance analysis and optimization of turbofan engines.

At present, the processing methods of stochastic uncertainty can be divided into two categories. One is to suppress the adverse effects of uncertainty through the control models, treat various uncertainties as stochastic disturbances and reduce the impact of stochastic uncertainty on the system performance as much as possible by designing a robust control law, so that the engine can better track the control commands and meet the required performance [25]. For example, the robust gain-scheduling control is used to eliminate the stochastic uncertainty arising from component degradation [26]. Model reference adaptive control and robust adaptive fault-tolerant control are also used to restrain uncertainty effects [27, 28]. Active disturbance rejection control is applied to reduce the uncertainty effects through the nonliner state observer [29]. Aiming at the strong uncertainty, the multivariable H-infinity robust control method is also designed in the current research [30]. The control-based methods reduce the influence of uncertainty on engine performance from the perspective of compensating control inputs, but which are difficult to optimize engine performance parameters by using the uncertainty influences.

The second method is to adjust the performance parameters and cycle parameters through the uncertainty quantification [31, 32]. At present, the methods of uncertainty quantification mainly include probability method, interval analysis method, surrogate model method and so on. The essence of the probability method is to solve the probability distributions of system responses by giving the probability distribution of uncertainty. The impact of advanced engine technology on fuel combustion and emission reduction is evaluated by the probability statistics [33]. Considering the uncertainties of component efficiency, flow rate and mechanical design variables, the engine performance is given in the form of a cumulative distribution function [34]. In addition, Monte Carlo simulation is also used to establish the probability model of engine performance design and quantify the impact of component performance uncertainty on the overall performance through the simulation experiments [35, 36]. The essence of the interval analysis method is to solve the various intervals of system responses by giving the variation interval of uncertainty. For example, the interval analysis is used to analyze the difference of the influence of component performance deviation on the system performance [37]. Surrogate models are data-based uncertainty analysis methods developed in recent years. It directly establishes a model with uncertainty as inputs and system performance as outputs to analyze the uncertainty influences. The reliability evaluation function is

established by generating a countermeasure network and Weibull distribution to realize the estimation of performance reliability [38]. The linear substitution model developed based on the least square method is used to quickly quantify uncertainty [21, 39].

Although these methods well consider the uncertainty from the application level, there are still some problems needing to be solved. The methods restraining the uncertainty influences by designing robust control law are developed from the perspective of compensating control commands, which fails to consider uncertainty in the performance optimization. Moreover, the methods proposed from the perspective of control cannot analyze the uncertainty influence characteristics on the thermodynamic parameters and performance parameters, which is not more beneficial to improving the engine performance. The uncertainty quantitative analyses based on probability methods face the cumbersome calculations. Interval analysis methods only analyze the change interval of uncertainty influences, but cannot determine the distribution features. The two quantitative methods based on the statistical analysis rely heavily on the number of simulations, they are difficult to be widely used in engine performance optimization and design due to high calculation cost and imprecise analysis results. The surrogate models still need to generate many uncertain samples to ensure the model accuracy, it still faces the problem of high calculation cost.

Aiming at two limitations existing in the existing methods, one is that the accurate quantitative analysis method is not found for the stochastic responses of engine thermodynamic state parameters and performance parameters and the other is that the uncertainty influence is hardly considered in the performance design, and the robust optimization method is not established to reduce the uncertainty influence, this paper focuses on the characteristics of strong nonlinearity and high uncertainty of turbofan engines. The stochastic response features under the stochastic excitations are studied through the stochastic dynamics model, which skillfully combines the nonlinear dynamics mechanism, uncertainty and the local and global response characteristics [40]. Stochastic dynamics is the most suitable method to analyze the influences of uncertainties on engine systems. At present, stochastic dynamics is widely used in the engineering fields. The stochastic dynamics accurately predicts the engine performance by fully considering the component uncertainties caused by the manufacturing process [41]. Stochastic dynamics is used to study the sensitivity of trains to the track geometry uncertainty [42]. The typical stochastic resonance phenomenon in stochastic dynamics is used to enhance the early weak signal features [43, 44]. The role of potential well depth and width on stochastic resonance driven by colored noise is discussed and evaluated [45]. Moreover, stochastic dynamics is also used for adaptive denoising for strong noisy images to improve the signal-to-noise ratio [46]. In addition, the nonlinear dynamics method is also used to analyze the combustion characteristics of the engine under an uncertain environment [47, 48]. In deep learning, stochastic dynamics is used in the reinforcement learning of nonlinear dynamics systems subject to additive stochastic uncertainty to ensure the system safety [49]. A new computational framework for stochastic manifolds is realized by differential geometry construction, stochastic dynamics and deep learning [50].

For the turbofan engines with multi-source uncertainties, the uncertainty impacts on the engine performance are usually difficult to accurately analyze due to the nonlinear actuation process. They are even more difficult to consider these uncertainties in the performance optimization and design. Stochastic dynamics is a potential method to solve the influence analyses of multi-source uncertainties, but related applications have not been found in turbofan engines. In this paper, the stochastic response analysis is realized by establishing the stochastic dynamics model to quantify the uncertainty influences. Then, the robust optimization method of engine performance is reported under the constraints of stochastic response distribution characteristics. Compared with other methods, the proposed robust optimization method has three obvious advantages. First, the stochastic dynamics model for analyzing the influence of uncertainty derived from the nonlinear dynamics equations does not need to be re-deduced at different operating points, and the corresponding stochastic dynamics model is established only by determining the coefficient matrices at different operating points. Secondly, the established stochastic dynamics model can simultaneously analyze the influences of multi-source uncertainties on the component state parameters and system performance based on the full-dimensional state variables, which is different from other methods that only analyze the

influence of uncertainty on the system performance. Thirdly, stochastic response distributions of different state parameters can be obtained by onetime calculation, which greatly reduces the calculation cost and has strong adaptability to practical applications.

The contents are arranged as follows: Sect. 2 derives the stochastic dynamics model to analyze the stochastic responses of engine systems. Section 3 analyzes the influences of actuator uncertainties on the stochastic responses of thermodynamic parameters and performance parameters. Section 4 establishes a robust optimization method based on the stochastic dynamics model to optimize engine performance. The main conclusions are given in Sect. 5.

2 Uncertainty influence analysis method

In this section, aiming at the nonlinear dynamics process of turbofan engines, a stochastic dynamics model for uncertainty influence analysis is established by using the knowledge of stochastic dynamics for the first time. Through mechanism derivation, it provides a novel and reliable method for rapid quantitative analysis of the influence of specific uncertainty on high-dimensional state parameters and performance parameters. A typical turbofan engine usually consists of the fan (F), compressor (C), combustion chamber (CC), high-pressure turbine (HPT), low-pressure turbine (LPT), afterburner (AB) and other key components. The schematic of the turbofan engine and its typical station numbering are shown in Fig. 1. The traditional mechanism modeling process of a turbofan engine can be found in Ref. [51].

The nonlinear dynamics process of a turbofan engine can be expressed as the following form [52, 53]:

$$\dot{\boldsymbol{x}}(t) = f(t,\boldsymbol{x}) + G(t,\boldsymbol{x})\boldsymbol{u}(t) \tag{1}$$

where $\boldsymbol{x}(t)$ represents the state variables. $f(t,\boldsymbol{x})$ represents the nonlinear function related to the system states. $G(t,\boldsymbol{x})$ represents the input function related to the system states. $\boldsymbol{u}(t)$ denotes the system inputs. Equation (1) describes the dynamics responses.

The actuators are mainly composed of mechanical parts and are used to execute the control commands. There are inevitable errors in the manufacturing and assembly process of mechanical parts, coupled with the wear caused by long-term actuation, resulting in a certain deviation between the actual outputs of the actuators and the control commands. We regard thess deviations as uncertainties in the actuating process of actuators. They make the state parameters and performance parameters show larger stochastic responses, which may cause adverse consequences in practical applications. The faults of actuators are not considered in here. When the input $\boldsymbol{u}(t)$ contains uncertainty, it is assumed that the state parameters consist of two parts. One part is the system state nominal value without stochastic interferences in a stable operation state, and the other part is the stochastic interferences caused by uncertainties, such as Eq. (2).

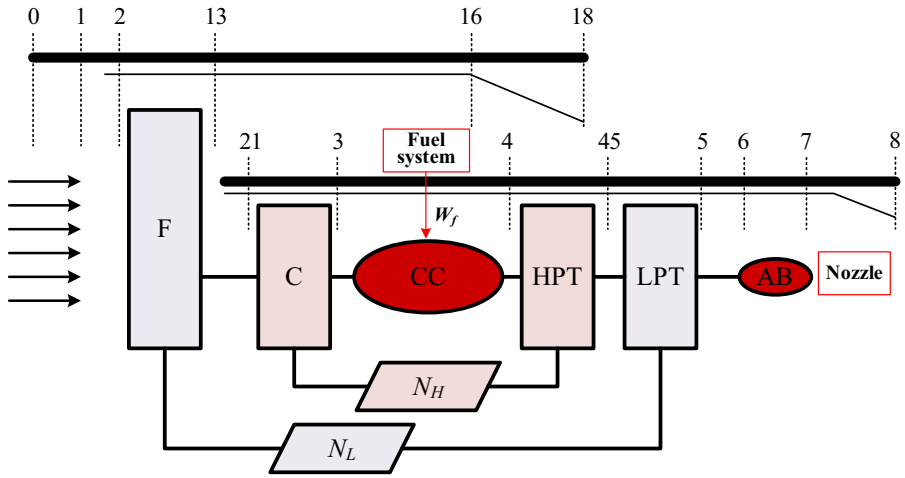

Fig. 1 Schematic of the turbofan engine and its typical station numbering

$$\boldsymbol{x} = \boldsymbol{x}_0 + \Delta \boldsymbol{x}\boldsymbol{u} = \boldsymbol{u}_0 + \Delta \boldsymbol{u} \tag{2}$$

where $\Delta \boldsymbol{u}$ denotes the stochastic uncertinties in inputs. $\Delta \boldsymbol{x}$ denotes the stochastic responses of the state variables. When the functions $f(t,\boldsymbol{x})$ and $G(t,\boldsymbol{x})$ are differentiable at the stable operation point $(\boldsymbol{x}_0, \boldsymbol{u}_0)$, Eq. (3) always holds in the neighborhood $U(\boldsymbol{x}_0, \boldsymbol{u_0})$.

$$\begin{aligned} f(t,\boldsymbol{x}) &= f(t,\boldsymbol{x}_0) + \frac{\partial f}{\partial \boldsymbol{x}_{\boldsymbol{x}_0}} \Delta \boldsymbol{x} + o(\Delta \boldsymbol{x}) \\ G(t,\boldsymbol{x}) &= G(t,\boldsymbol{x}_0) + \frac{\partial G}{\partial \boldsymbol{x}_{\boldsymbol{x}_0}} \Delta \boldsymbol{x} + o(\Delta \boldsymbol{x}) \end{aligned} \tag{3}$$

where $o(\Delta \boldsymbol{x})$ represents the infinitesimal quantity. Substituting Eq. (3) into Eq. (1) to obtain

$$\begin{aligned} \dot{\boldsymbol{x}}_0 + \Delta \dot{\boldsymbol{x}} = f(t,\boldsymbol{x}_0) + \frac{\partial f}{\partial \boldsymbol{x}}|_{\boldsymbol{x}_0} \Delta \boldsymbol{x} + o(\Delta \boldsymbol{x}) + [G(t,\boldsymbol{x}_0) \\ + \frac{\partial G}{\partial \boldsymbol{x}}|_{\boldsymbol{x}_0} \Delta \boldsymbol{x} + o(\Delta \boldsymbol{x})](\boldsymbol{u}_0 + \Delta \boldsymbol{u}) \end{aligned} \tag{4}$$

It is known from Eq. (2) that the stable operation point $(\boldsymbol{x}_0, \boldsymbol{u}_0)$ also satisfies Eq. (1), which is

$$\dot{\boldsymbol{x}}_0(t) = f(t,\boldsymbol{x}_0) + G(t,\boldsymbol{x}_0)\boldsymbol{u}_0(t) \tag{5}$$

Equation (4) subtracts Eq. (5) to obtain the linearized system equation describing the influences of stochastic uncertainties on system states around the stable operation point, as expressed as

$$\begin{aligned} \Delta \dot{\boldsymbol{x}} = \frac{\partial f}{\partial \boldsymbol{x}}|_{\boldsymbol{x}_0} \Delta \boldsymbol{x} + o(\Delta \boldsymbol{x}) + G(t,\boldsymbol{x}_0)\Delta \boldsymbol{u} + \frac{\partial G}{\partial \boldsymbol{x}}|_{\boldsymbol{x}_0} \boldsymbol{u}_0 \Delta \boldsymbol{x} \\ + \frac{\partial G}{\partial \boldsymbol{x}}|_{\boldsymbol{x}_0} \Delta \boldsymbol{x} \Delta \boldsymbol{u} + o(\Delta \boldsymbol{x})(\boldsymbol{u}_0 + \Delta \boldsymbol{u}) \end{aligned} \tag{6}$$

Since $\Delta \boldsymbol{x}$ and $\Delta \boldsymbol{u}$ are smaller stochastic uncertainties, the term $\left\{\frac{\partial G}{\partial \boldsymbol{x}}|_{\boldsymbol{x}_0} \Delta \boldsymbol{x} \Delta \boldsymbol{u} + o(\Delta \boldsymbol{x}) + o(\Delta \boldsymbol{x})(\boldsymbol{u}_0 + \Delta \boldsymbol{u})\right\}$ is still a smaller stochastic quantity. If it is directly ignored, Eq. (6) only expresses the linear features near the stable operation point, which obviously does not conform to the dynamics characteristics of the engine system and also reduces the model accuracy. Noting that this term is only determined by the stochastic components $\Delta \boldsymbol{x}$ and $\Delta \boldsymbol{u}$, and $\Delta \boldsymbol{x}$ is the stochastic responses under the stochastic excitation $\Delta \boldsymbol{u}$, so this term can be uniformly expressed by $\Delta \boldsymbol{x}$. To study the influence of stochastic uncertainties on the system responses in a wider range, this term is simplified as the nonlinear term $\boldsymbol{F}(\Delta \boldsymbol{x})^2$, where $\boldsymbol{F}$ is a constant matrix, then Eq. (6) is transformed into

$$\Delta \dot{\boldsymbol{x}} = \left(\frac{\partial f}{\partial \boldsymbol{x}}|_{\boldsymbol{x}_0} + \frac{\partial G}{\partial \boldsymbol{x}}|_{\boldsymbol{x}_0} \boldsymbol{u}_0\right) \Delta \boldsymbol{x} + F(\Delta \boldsymbol{x})^2 + G(t,\boldsymbol{x}_0)\Delta \boldsymbol{u} \tag{7}$$

Equation (7) is a typical nonlinear stochastic differential system in which the system responses deviate from the stable states under stochastic excitations.

Let $\boldsymbol{A} = \left(\frac{\partial f}{\partial \boldsymbol{x}}|_{\boldsymbol{x}_0} + \frac{\partial G}{\partial \boldsymbol{x}}|_{\boldsymbol{x}_0} \boldsymbol{u}_0\right)$ and $\boldsymbol{B} = G(t,\boldsymbol{x}_0)$, and then, Eq. (7) is transformed into

$$\Delta \dot{\boldsymbol{x}} = \boldsymbol{A}\Delta \boldsymbol{x} + \boldsymbol{F}(\Delta \boldsymbol{x})^2 + \boldsymbol{B}\Delta \boldsymbol{u} \tag{8}$$

Equation (8) describes the stochastic responses $\Delta \boldsymbol{x}$ of state parameters under stochastic excitations $\Delta \boldsymbol{u}$. The coefficient matrices $\boldsymbol{A}$, $\boldsymbol{B}$ and $\boldsymbol{F}$ can be obtained by using the engine dynamic model and the small disturbance method to establish a nonlinear stochastic differential system representing the stochastic responses. However, it is difficult to be solved directly.

Equation (8) is a nonlinear stochastic differential equation, which is commonly treated by the equivalent linearization method in the stochastic dynamics, that is, the nonlinear stochastic differential Eq. (8) is replaced by equivalent linear stochastic differential equations. Now replacing the jth state variable in Eq. (8) with the following linear stochastic differential equation

$$(\Delta \dot{x})_j = A_j \Delta \boldsymbol{x} + B_j \Delta \boldsymbol{u} + \sum_{k=1}^{n} \alpha_{jk} (\Delta x)_k, j = 1, 2, \ldots, n. \tag{9}$$

where A_j and B_j represent the jth row elements in $\boldsymbol{A}$ and $\boldsymbol{B}$. $(\Delta x)_k$ denotes the kth state variable in Eq. (8). α_{jk} is the coefficient related to the kth state variable, Which is determined by the statistical minimum of the difference between nonlinear and linear stochastic differential equations. Substracting Eq. (8) from Eq. (9) yields

$$\delta = \sum_{j=1}^{n} \left[F_j (\Delta \boldsymbol{x})^2 - \sum_{k=1}^{n} \alpha_{jk} (\Delta x)_k \right] \tag{10}$$

Using the minimum mean square deviation criterion to obtain Eq. (11),

$$\frac{\partial}{\partial \alpha_{jk}} E\left[\delta^2\right] = 0, j, k = 1, 2, \ldots, n. \tag{11}$$

Substituting Eq. (10) into Eq. (11), the statistical characteristics of the equivalent linearization process are obtained, as displayed in Eq. (12).

$$E\left\{ (\Delta x)_k \sum_{j=1}^{n} \left[F_j (\Delta \boldsymbol{x})^2 - \sum_{k=1}^{n} \alpha_{jk} (\Delta x)_k \right] \right\} = 0 \tag{12}$$

α_{jk} can be solved by the iterative calculation and is recorded as $\boldsymbol{\alpha} = [\boldsymbol{\alpha_{jk}}]$, $\boldsymbol{\alpha}$ is an n-dimensional square matrix. Then, Eq. (13) can be obtained by combining Eq. (9) and substituting it into Eq. (7). This is a linear equivalent equation obtained by the equivalent linearization method in stochastic dynamics.

$$\Delta \dot{\boldsymbol{x}} = \left(\frac{\partial f}{\partial \boldsymbol{x}} |_{\boldsymbol{x}_0} + \frac{\partial G}{\partial \boldsymbol{x}} |_{\boldsymbol{x}_0} \boldsymbol{u}_0 + \boldsymbol{\alpha} \right) \Delta \boldsymbol{x} + G(t, \boldsymbol{x}_0) \Delta \boldsymbol{u} \tag{13}$$

Let $\boldsymbol{z} = \Delta \boldsymbol{x}$, $\boldsymbol{w}(t) = \Delta \boldsymbol{u}$, $\boldsymbol{H} = \frac{\partial f}{\partial \boldsymbol{x}} |_{\boldsymbol{x}_0} + \frac{\partial G}{\partial \boldsymbol{x}} |_{\boldsymbol{x}_0} \boldsymbol{u}_0 + \boldsymbol{\alpha} = \boldsymbol{A} + \boldsymbol{\alpha}$, $\boldsymbol{B} = G(t, \boldsymbol{x}_0)$. For stochastic differential Eq. (13), we can obtain the expectation and variance of stochastic responses $\Delta \boldsymbol{x}$, as Eq. (14).

$$\overline{\boldsymbol{z}} = E[\boldsymbol{z}], \boldsymbol{D}(t) = E\{[\boldsymbol{z} - \overline{\boldsymbol{z}}][\boldsymbol{z} - \overline{\boldsymbol{z}}]^T\} \tag{14}$$

Assume that the stochastic uncertainties are the Gaussian white noise, because the distribution characteristics of Gaussian white noise accord with most engineering application assumptions, and the stochastic differential equation excited by Gaussian white noise is easier to be solved. Equation (13) is deduced that

$$\dot{\boldsymbol{D}}(t) = \boldsymbol{H}\boldsymbol{D}(t) + \boldsymbol{D}(t)\boldsymbol{H}^T + \boldsymbol{B}\boldsymbol{P}\boldsymbol{B}^T \tag{15}$$

where $\boldsymbol{P}$ is the spectral densities of stochastic excitations.

The stochastic vector samples $\boldsymbol{w}(t)$ of stochastic uncertainties can be expressed as

$$\boldsymbol{w}(t) = \boldsymbol{R}\boldsymbol{S}(t), \frac{d\boldsymbol{S}(t)}{dt} = 0 \tag{16}$$

where $\boldsymbol{S}(t)$ is a stationary stochastic sample vector independent of time and $\boldsymbol{R}$ represents the observation matrix of the intensity of the stochastic sample vector. Then the stochastic differential equation in Eq. (13) is transformed into

$$\begin{bmatrix} \dot{\boldsymbol{z}}(t) \\ \dot{\boldsymbol{S}}(t) \end{bmatrix} = \begin{bmatrix} \boldsymbol{H} & \boldsymbol{B}\boldsymbol{R} \\ 0 & 0 \end{bmatrix} \begin{bmatrix} z(t) \\ S(t) \end{bmatrix} \tag{17}$$

Let $\boldsymbol{M} = \begin{bmatrix} \boldsymbol{H} & \boldsymbol{B}\boldsymbol{R} \\ 0 & 0 \end{bmatrix}$, and the covariance matrix is defined as

$$\begin{aligned} \boldsymbol{D}(t) &= \begin{bmatrix} D_{zz} & D_{zs} \\ D_{sz} & D_{ss} \end{bmatrix} \\ &= E\left[\begin{Bmatrix} \Delta z \\ \Delta w \end{Bmatrix} \begin{Bmatrix} (\Delta z)^T & (\Delta \boldsymbol{w})^T \end{Bmatrix} \right] \end{aligned} \tag{18}$$

The covariance matrix differential equation is obtained by Eqs. (13, 15, 17 and 18), as Eq. (19).

$$\dot{\boldsymbol{D}}(t) = \boldsymbol{M}\boldsymbol{D}(t) + \boldsymbol{D}(t)\boldsymbol{M}^T \tag{19}$$

This covariance matrix differential equation describes the variances of thermodynamic parameters and the covariances between two thermodynamic parameters when the engine system is subjected to stochastic uncertainties, which provides quantitative stochastic responses of the engine system. The design point of the engine system is also a stable operation point, which also satisfies Eqs. (1 and 5).

3 Actuator uncertainty influence analysis

Based on the stochastic dynamics model derived in Sect. 2, a full-dimensional nonlinear state-space model is established to determine the coefficient matrices in Eq. (8). Then, the stochastic responses of thermodynamic parameters and system performance are further analyzed by considering actuator uncertainties, which provides the quantitative analysis results of uncertainty influences for the performance optimization.

3.1 Nonlinear turbofan engine model

The establishment of the nonlinear state-space model of a turbofan engine is divided into two steps. Firstly, the full-dimensional linear state-space model at the stable operation point is established, and then, the nonlinear term is considered to modify the linear model, to further establish a nonlinear state-space model. In the engine performance control, based on the engine component level dynamic model, the coefficient matrices $\boldsymbol{A}$ and $\boldsymbol{B}$ in the linear model are

obtained by applying the small disturbance method. The established linear model is shown in Eq. (20) [54].

$$\Delta\dot{\boldsymbol{x}} = \boldsymbol{A}\Delta\boldsymbol{x} + \boldsymbol{B}\Delta\boldsymbol{u} \tag{20}$$

where thermodynamic state parameters $\boldsymbol{x} = [N_L, N_H, P_{13}, P_3, T_4, P_{45}, T_{45}, P_5, P_7]^{\boldsymbol{T}}$, model inputs $\boldsymbol{u} = [w_f, A_8]^{\boldsymbol{T}}$, and $\boldsymbol{A} \in R_{9\times9}$, $\boldsymbol{B} \in R_{9\times2}$. The parameter descriptions are given in Table 1. To analyze the influence of stochastic uncertainty, each engine component selects a state parameter to construct a full-dimensional state-space model. The main fuel flow rate w_f and nozzle throat area A_8 are usually used in the closed-loop control of aero-engines to control low-pressure rotor speed N_L and high-pressure rotor speed N_H. The low-pressure and high-pressure shafts connect the whole engine system, so the fuel system and nozzle are selected as actuators, with w_f and A_8 as input variables. The small disturbance method is used to obtain the coefficient matrices $\boldsymbol{A}$ and $\boldsymbol{B}$; that is, the step disturbance is applied to the state parameters $\boldsymbol{x}$ and control inputs $\boldsymbol{u}$, respectively, at the stable operation point, while the other state parameters and input parameters remain unchanged. And then the engine dynamic model is used for calculation to obtain the derivatives of the state parameters under the corresponding step disturbance at the current time. The coefficient matrices $\boldsymbol{A}$ and $\boldsymbol{B}$ are obtained by calculating the ratio of the derivatives of the state parameters to the small disturbances.

The linear model extracted at the stable operating point only approximately describes dynamic characteristics in a small neighborhood. In this paper, the general nonlinear term $f(\Delta\boldsymbol{x}) = \boldsymbol{F}[\Delta\boldsymbol{x}]^2$ is introduced to modify the linear state-space model to improve the model accuracy and broaden the working range of the model. The nonlinear state-space model is shown in Eq. (21).

$$\Delta\dot{\boldsymbol{x}} = A\Delta\boldsymbol{x} + B\Delta\boldsymbol{u} + f(\Delta\boldsymbol{x}) \tag{21}$$

The system model considering nonlinearity is consistent with Eqs. (7 and 8), which essentially describe the responses of thermodynamic parameters under small stochastic disturbance.

Next, the calculation method of nonlinear coefficient matrix $\boldsymbol{F}$ is introduced. The step response data of M groups of thermodynamic parameters under the step changes of fuel flow rate and nozzle area are obtained through the traditional dynamic model [51]. This dynamic model is established through mechanism equations of engine systems. The contradiction Eq. (22) is constructed to constrain the calculation process.

$$\begin{aligned}\boldsymbol{v}(t_i)_j = {} & [\Delta\dot{\boldsymbol{x}}(t_i)_j - A\Delta\boldsymbol{x}(t_i)_j - B\Delta\boldsymbol{u}(t_i)_j]^{\boldsymbol{T}} \\ & - \left[\Delta\boldsymbol{x}^2(t_i)_j\right]^{\boldsymbol{T}}\boldsymbol{F}^{\boldsymbol{T}}\end{aligned} \tag{22}$$

where t_i is the sampling time of the dynamic model and $j = 1, 2, \ldots, M$. The coefficient matrix $\boldsymbol{F}$ is solved by the least square algorithm. $\boldsymbol{v}(t_i)_j$ is used to evaluate the solution accuracy. When $\frac{1}{M}\sum_{j,i}\boldsymbol{v}(t_i)_j$ is less than the setting error, then the solved $\boldsymbol{F}$ meets the accuracy requirements. In fact, the cumulative error in the process of calculating the coefficient matrices $\boldsymbol{A}$ and $\boldsymbol{B}$ is eliminated by the nonlinear term coefficient $\boldsymbol{F}$.

Based on the full-dimensional nonlinear state-space model, we take 1.2% of the steady-state value of each thermodynamic parameter and input parameter as the small disturbance and apply it to the traditional dynamic model to obtain coefficient matrices $\boldsymbol{A}, \boldsymbol{B}and\boldsymbol{F}$. When solving $\boldsymbol{F}$, the response data obtained under 10 groups of step excitations of fuel flow rate

Table 1 Thermodynamic parameter descriptions

Parameters	Descriptions	Parameters	Descriptions
N_L	Rotation speed of the low-pressure shaft	T_{45}	Outlet temperature of HPT
N_H	Rotation speed of the high-pressure shaft	P_5	Outlet pressure of LPT
P_{13}	Outlet pressure of fan	P_7	Outlet pressure of afterburner
P_3	Outlet pressure of the compressor	w_f	Fuel flow rate
T_4	Turbine inlet temperature	A_8	Nozzle area
P_{45}	Outlet pressure of HPT		

and nozzle area is used, and the average error $\frac{1}{M}\sum_{j,i}\boldsymbol{v}(t_i)_j$ is 0.0027, which shows that the nonlinear state-space model well reflects the nonlinear characteristics of engine systems. Figure 2 shows the dynamic responses of the traditional dynamic model and nonlinear state-space model (Eq. (21)) when the step excitations of fuel flow rate are 1%, 1.5% and 2%. The results indicate that the nonlinear state-space model accurately describes the dynamic characteristics. It provides a high-accuracy model for the stochastic response analysis of turbofan engines excited by actuator uncertainties.

3.2 Stochastic responses analyses

In this section, the purpose of analyzing the stochastic responses of thermodynamic parameters based on the stochastic dynamic model is not to eliminate the influence of uncertainty, but to analyze the distribution characteristics of thermodynamic parameters and performance parameters in the presence of actuator uncertainties, so as to use these distribution characteristics to design higher-performance engine parameters.

Based on the coefficient matrices $\boldsymbol{A}$, $\boldsymbol{B}$ and $\boldsymbol{F}$ obtained in Sect. 3.1, the complete expression shown in Eq. (21) is established, and then, the covariance matrix differential equation shown in Eq. (19) is established. The stochastic influences of actuator uncertainties on the thermodynamic parameters are solved through Eq. (19), in which the elements on the main diagonal of $\boldsymbol{D}(t)$ represent the variances of thermodynamic parameters and the other elements represent the covariances between two thermodynamic parameters. First, we need to determine the matrix $\boldsymbol{M}$, in other words, determining matrices $\boldsymbol{\alpha}$ and $\boldsymbol{R}$. Matrix $\boldsymbol{\alpha}$ is obtained by taking Eq. (12) as the

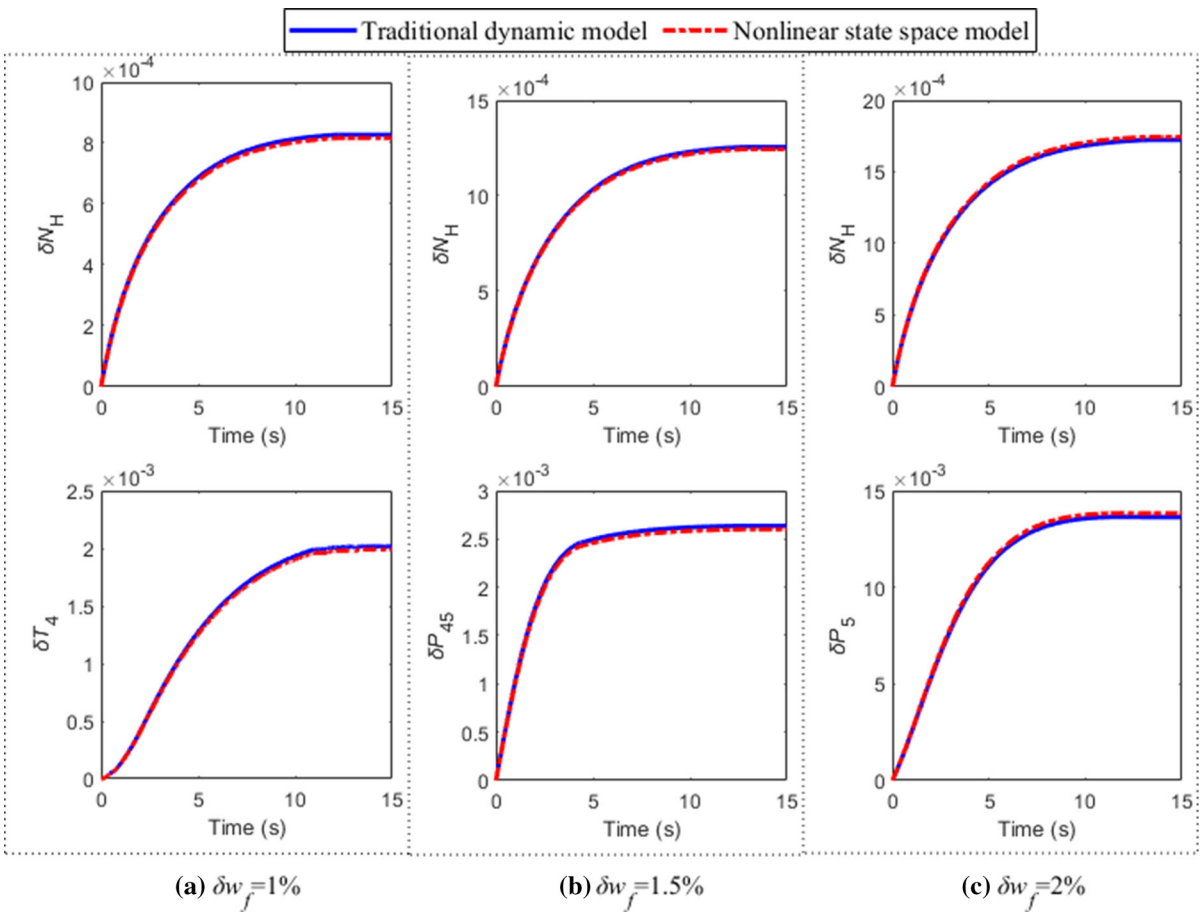

Fig. 2 Dynamic responses of the traditional dynamic model and nonlinear state-space model

constraint condition and then guessing the initial values and iterative calculation. $\boldsymbol{R}$ is the observation matrix of stochastic uncertainty intensities, $\boldsymbol{R} \in R_{2\times 2}$. According to Eq. (16), the uncertainties of fuel system and nozzle is defined as follows

$$\boldsymbol{w}(t) = \begin{bmatrix} R_1 & 0 \\ 0 & R_2 \end{bmatrix} \begin{bmatrix} S_1(t) \\ S_2(t) \end{bmatrix} \tag{23}$$

$\boldsymbol{S}(t)$ is a stationary stochastic vector. In general, assuming that $\boldsymbol{S}(t)$ obeys the normal distribution in the specified interval $[-m, m]$, the benchmark uncertainties of actuators are expressed as

$$\begin{cases} S_1(t) = normrnd\_w_f(0, \sigma, 1, N) \\ S_2(t) = normrnd\_A_8(0, \sigma, 1, N) \end{cases}, \boldsymbol{\sigma} = \frac{\boldsymbol{m}}{\boldsymbol{2.58}} \tag{24}$$

where, normrnd$(0, \sigma, 1, N)$ indicates a stochastic vector (1 row and N columns) with the normal distribution (0 mean value and σ standard deviations). $m = 0.1$. R_1 and R_2 measure the uncertainty intensities of fuel system and nozzle on the basis of benchmark uncertainties, which represent the magnitudes of uncertainties.

(1) Variance response analysis

In this paper, we refer to the main performance parameters of F119 turbofan engine. The main performance parameters of F119 turbofan engine are listed in Table 2.

Figure 3 shows the variance evolution trends of thermodynamic parameters with the operating time when they are affected by the actuation uncertainties of fuel system and nozzle. The uncertainty intensities are set as R1 = 2 and R2 = 2. In general, the variances of all thermodynamic parameters show a consistent change trend from small to large. This trend that the parameter variance gradually increases with the increase in the time reflects the cumulative influence of uncertainties and the amplification effect of nonlinearity. In practical applications, this gradually increasing evolution trend is broken by the controller and the switching of engine operating conditions, so it does not cause serious harm to the engine system, but

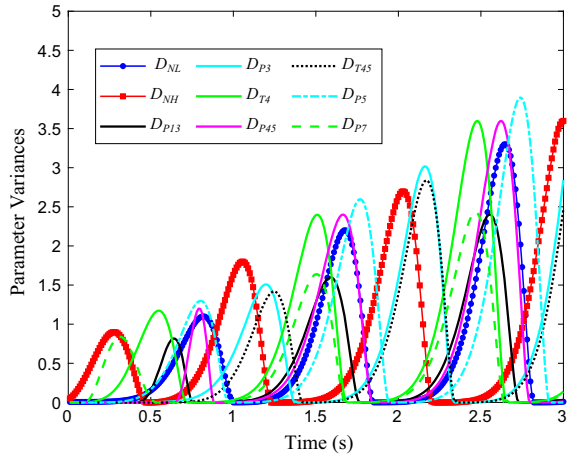

Fig. 3 Variance evolution trends of thermodynamic parameters under actuator uncertainties

will affect the working performance. In addition, the evolution process of variance has obvious peak-valley characteristics, which are mainly caused by the periodic rotation features of the engine itself. Figure 3 directly shows that the actuator uncertainties have a great interference on the thermodynamic parameters, which should be fully considered in the engine performance optimization design.

Based on the results shown in Fig. 3, the influence laws of actuator uncertainties are further analyzed. Here, the first arrival time (FAT) and first duration time (FDT) are defined to describe the influences of actuator uncertainties on thermodynamic parameters. In practice, we hope that the uncertainty influence is small enough, and the stochastic responses of thermodynamic parameters will not be continuously amplified with the changes of engine operating conditions. Therefore, we selected the first variance arch peak of each thermodynamic parameter in Fig. 3 for analysis. The FAT and FDT are defined as follows

$$\begin{aligned} \mathrm{FAT}_i &= t^i_{\mathrm{Var-Peak}} \\ \mathrm{FDT}_i &= t^i_{\mathrm{Var}\to 0\ \mathrm{After-FAT}} - t^i_{\mathrm{Var}\to 0\ \mathrm{Before-FAT}} \end{aligned} \tag{25}$$

Table 2 Main performance parameters of F119 turbofan engine

Total pressure ratio	Turbine inlet temperature (K)	Bypass ratio	Maximum thrust (kN)
35	1850–1950	0.3	155.7

where i represents the ith thermodynamic parameter. *Var-Peak* represents the first variance peak value. FAT reflects the sensitivity of the component operating state to the actuator uncertainties. FDT reflects the influence degree of the actuator uncertainties on the component operation state.

Figure 4 shows the comprehensive analysis results of stochastic responses. Through the comprehensive analyses of the variances, FATs and FDTs, the following conclusions are obtained: (I) The actuator uncertainties has a greater impact on the core engine components (dashed box) than other components. (II) The high-speed shaft is most sensitive to the actuator uncertainties, but the low-speed shaft is greatly affected due to larger variance and longer duration time. (III) The compressor outlet pressure P_3 is slow to perceive the actuator uncertainties, but it is most adversely affected due to the greatest variance and the longest duration time. The outlet temperature T_{45} of the high-pressure turbine also shows a similar phenomenon, which is caused by the accumulation of stochastic responses at the high-pressure turbine outlet. (IV) From the main combustion chamber outlet to the afterburner chamber outlet (arrow), the sensitivity to the actuator uncertainties decreases first and then increases, but the uncertainty influence degree increases first and then decreases, which shows the opposite trend. This is because the insensitive thermodynamic parameters to actuator uncertainties cannot eliminate the cumulative influence with the help of the changing operating conditions.

Figure 4 shows the comprehensive analysis results under the same uncertainty intensities. Figure 5 further analyzes the stochastic responses when there is only the fuel system actuation uncertainty or nozzle actuation uncertainty. The results show that: (I) Without considering the fuel system actuation uncertainty (R1 = 0), the nozzle actuation uncertainty intensities have almost no effect on the distribution characteristics of all thermodynamic parameters, namely the variance curves under different intensities coincide completely, and it has the same effects on the parameters of N_L, P_3, T_4 and P_5, and same effects on the parameters N_H, P_{13}, P_{45} and P_7. (II) Without considering the nozzle actuation uncertainty (R2 = 0), the fuel system uncertainty intensities have little impact on the parameters of N_L, P_3, T_4 and P_5, and have a greater impact on the parameters N_H, P_{13}, P_{45} and P_7; namely, under different uncertainty intensities, the variance curves of N_L, P_3, T_4 and P_5 have very little difference, while the variance curves of N_H, P_{13}, P_{45} and P_7 decreased with the decrease of R1. (III) The sensitivities of all thermodynamic parameters to nozzle uncertainty are higher than those of the fuel system uncertainty (identified by the vertical dotted line in Fig. 5). (IV) For N_L, P_3, T_4 and P_5, the influences of nozzle uncertainty are greater than those of fuel system uncertainty, but the differences of peak variances are smaller. The maximum variance deviation is only 0.15. For N_H, P_{13}, P_{45} and P_7, the influences of fuel system uncertainty are greater than those of nozzle uncertainty, and the differences of peak variances are larger. The maximum variance deviation is 0.52. Therefore, the influence of the fuel system uncertainty on thermodynamic parameters is the greatest.

Further, we analyzed the stochastic responses of thermodynamic parameters under the two actuator uncertainties, as shown in Fig. 6. For N_L, P_3, T_4 and P_5, when the fuel system uncertainty is maximum and unchanged (R1 = 3), the variance of the thermodynamic parameter increases with the increase of R2. Then, R2 remains unchanged, and the variances of the thermodynamic parameter continue to increase to the

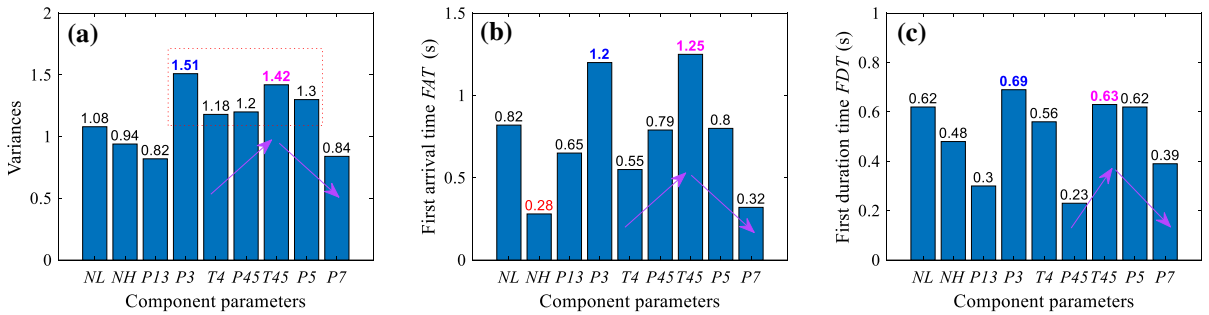

Fig. 4 Comprehensive analyses of stochastic responses of thermodynamic parameters under actuator uncertainties

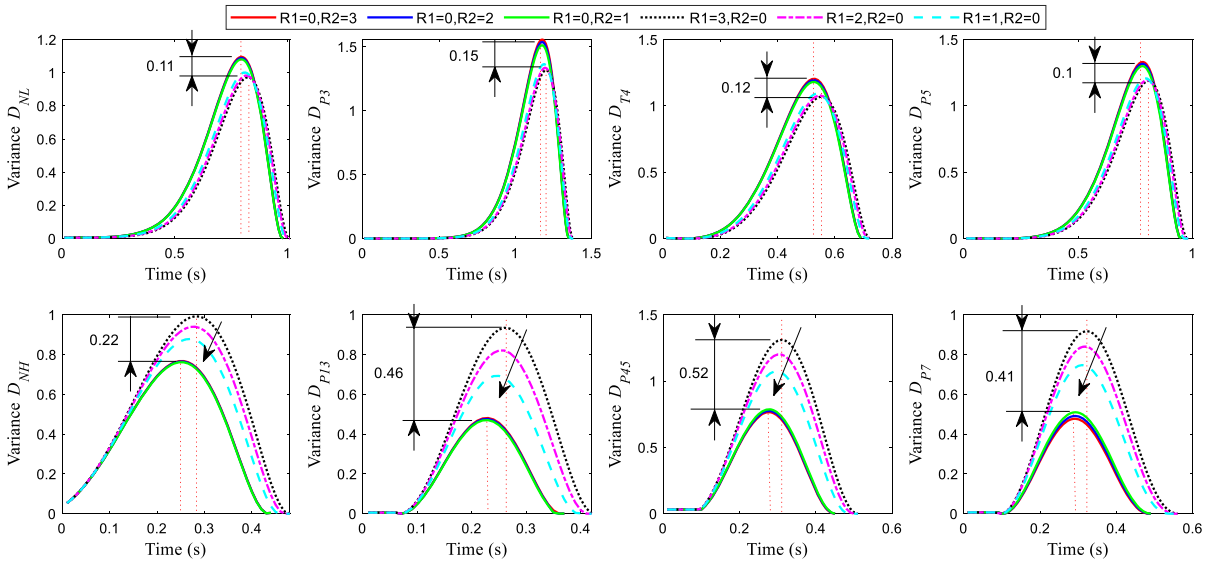

Fig. 5 Comparisons of stochastic responses of thermodynamic parameters under independent fuel system uncertainty or nozzle uncertainty

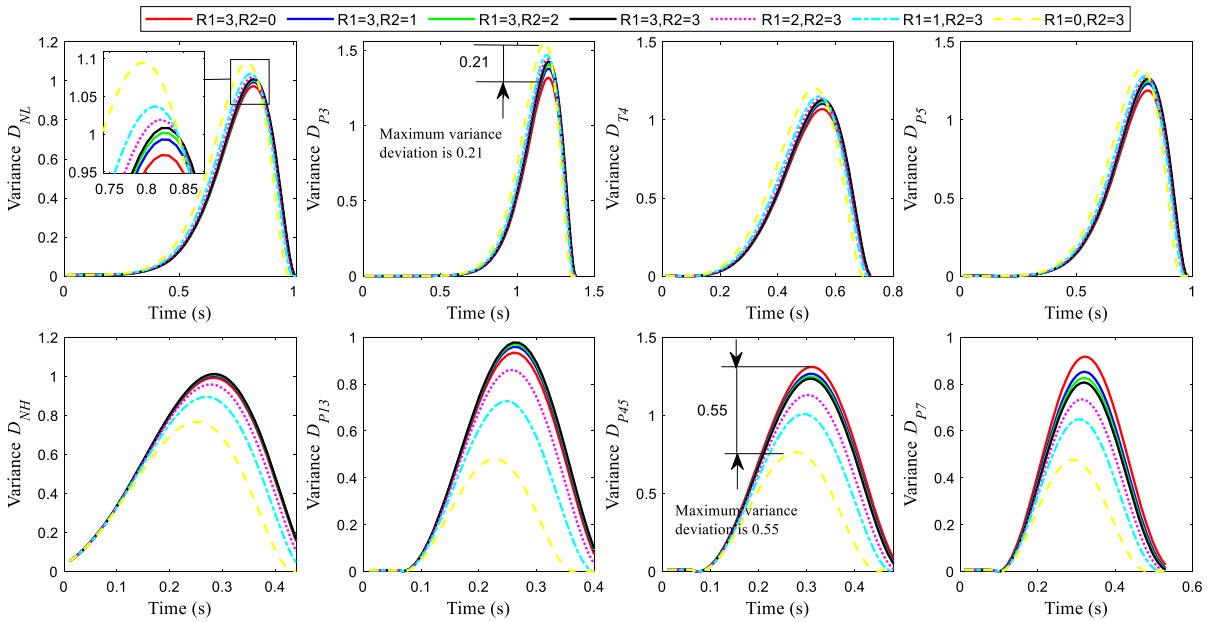

Fig. 6 Comprehensive influence analyses of two actuator uncertainties on stochastic responses of thermodynamic parameters

maximum with the decrease of R1. It shows that the stochastic response characteristics of these thermodynamic parameters are greatly affected by the nozzle actuation uncertainty, but the maximum variance deviation is only 0.21. It is consistent with the conclusion in Fig. 5. For N_H, P_{13}, P_{45} and P_7, when the nozzle uncertainty is maximum and unchanged (R2 = 3), the parameter variance increases with the increase of R1. Then, R1 remains unchanged, and the parameter variances continue to increase to the maximum with the decrease of R2. It shows that the stochastic response characteristics of these thermodynamic parameters are greatly affected by the fuel system, and the maximum variance deviation reaches

0.55. It is also consistent with the conclusion in Fig. 5. The comprehensive results show that the fuel system uncertainty is still the main factor affecting the stochastic response characteristics.

Figures 3, 5 and 6 analyze the evolution law of stochastic responses of thermodynamic parameters with time under different actuator uncertainty intensities. When R1 = R2 = 2, Fig. 7 shows the distribution characteristics of several key component parameters at the first peak variance. The maximum probability density corresponds to the mean value of the stochastic response distribution. In Fig. 7, when there are actuator uncertainties, the real operating states of engine components are normal distributions, indicating that the actuator uncertainty has a great impact on the engine operating states. Further, the influences of actuator uncertainties with different intensities on the engine performance are analyzed, as Fig. 8. The performance parameters F and SFC are calculated through the steady-state model when considering the uncertainties of fuel system and nozzle under the stable operation.

The increased uncertainties lead to the decrease in the thrust and the increase in the specific fuel consumption (SFC). The greater the uncertainty, the smaller the probability densities of thrust and SFC, indicating that the stochastic responses of the engine performance are more dispersed. The results are shown in Table 3. When only considering the fuel system uncertainty or nozzle uncertainty, compared with the nozzle uncertainty, the fuel system uncertainty reduces the thrust by 2.9 kN and increases the SFC by 0.016 k/(kg·h). The fuel system uncertainty has a greater impact on the engine performance, which is consistent with the previous conclusions.

(2) Covariance response analysis

In part (1), the variances of thermodynamic parameters are analyzed. The covariances between two thermodynamic parameters are also obtained by Eq. (19). Covariance represents the overall error of two parameters and describes the change degrees of stochastic responses in the same or opposite direction. Positive covariance indicates that the stochastic response trends of two thermodynamic parameters are consistent, while negative covariance indicates that the stochastic response trends are opposite. The greater the covariance, the greater the change degree of two parameters in the same or opposite direction.

Figure 9 analyzes the covariance evolution trends between different thermodynamic parameters with time when R1 = 2 and R2 = 2. The covariances between different parameters change alternately in the same direction and the opposite direction. It is because the stochastic responses of thermodynamic parameters present the normal distributions, resulting in the thermodynamic parameters being greater than the theoretical design value at the same time or one is greater than and the other is less than the theoretical design value. In addition, with the time accumulation,

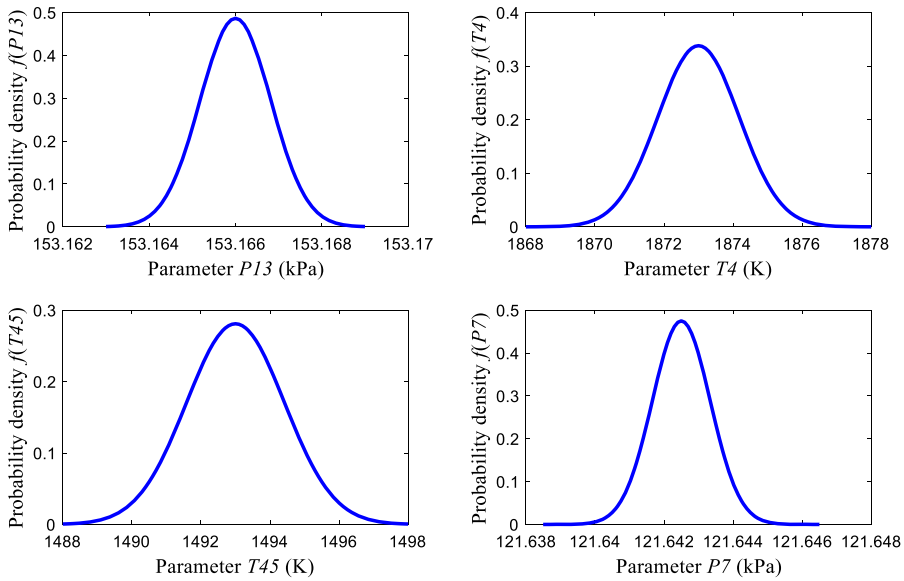

Fig. 7 Stochastic response characteristics of thermodynamic parameters under actuator uncertainties

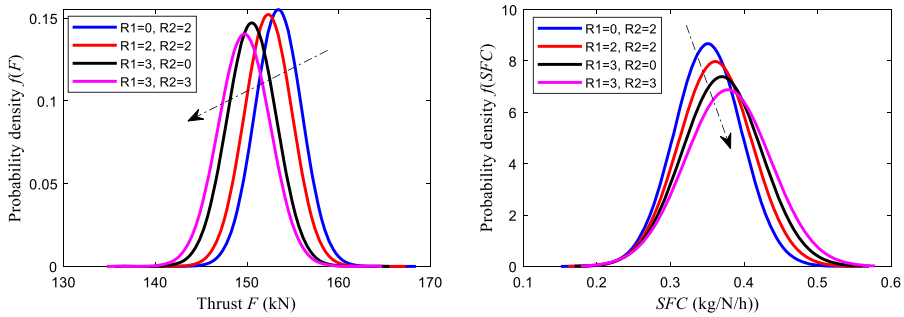

Fig. 8 Influences of actuator uncertainties with different intensities on the engine performance

Table 3 Effects of actuator uncertainties on thrust and SFC

Uncertainty	R1 = 0 R2 = 2	R1 = 2 R2 = 2	R1 = 3 R2 = 0	R1 = 3 R2 = 3
$f(F)$	0.1552	0.1523	0.1472	0.1401
Thrust F	153.4	152.3	150.5	149.7
$f(SFC)$	8.671	7.977	7.383	6.877
SFC	0.3518	0.3598	0.3678	0.3789

the covariance increases sharply, which indicates that when the engine operates for a long time under a stable operating state and the actuator has greater uncertainty, it will lead to a severe alternating trend in the same direction and in the opposite direction between the thermodynamic parameters, which may lead to serious instability of the engine system and seriously affect the engine performance. Therefore, the actuator uncertainties and the stochastic responses of thermodynamic parameters need to be considered in the performance optimization design stage of turbofan engines.

4 Engine performance robust optimization

4.1 Robust optimization method

The uncertainties of actuators are inevitable. We analyzed the influence characteristics of uncertainties on the thermodynamic parameters and performance parameters based on the stochastic dynamics model. We expect that the influences of uncertainty can be considered in the design stage of engine performance parameters, so that the designed performance parameters are less disturbed by uncertainties in the practical applications and make the engine performance more robust.

The performance robust optimization design considering actuator uncertainties is actually to optimize the design parameters of turbofan engines based on the stochastic response characteristics. For a turbofan engine, the design parameters usually include total pressure ratio π_{total}, bypass ratio B_r, main combustion chamber outlet temperature T_4 and afterburner outlet temperature T_7. Under the constraints of the stochastic response distribution characteristics of thermodynamic parameters, the Newton interior-point method is used to optimize the design parameters. When the iteration point is close to the feasible region boundary, the fitness function increases sharply to prevent the iteration point from crossing the boundary to obtain the optimal solutions; therefore, it has high optimization efficiency and global optimization ability [55]. The robust optimization model is established as follows

$$\text{Optimization Target}: \pi_{\text{total}},\ B_r,\ T_4,\ T_7 \tag{26}$$

$$\begin{aligned}&\text{Fitness function}: \left[F_{\text{optimized}},\ \text{SFC}_{\text{optimized}}\right]\\&= f(\pi_{\text{total}}, B_r, T_4, T_7, \mathbf{inputs})\\&\text{Fitness} = \min\left\{\omega_1 \frac{F_{\text{original}}}{F_{\text{optimized}}} + \omega_2 \frac{\text{SFC}_{\text{optimized}}}{\text{SFC}_{\text{original}}}\right\}\end{aligned} \tag{27}$$

$$\begin{aligned}&s.t.\ \boldsymbol{lb} \le [\pi_{total},\ B_r,\ T_4,\ T_7] \le \boldsymbol{ub}\\&\boldsymbol{Paras}_0 - 3\boldsymbol{\sigma} \le \boldsymbol{Paras} \le \boldsymbol{Paras}_0 + 3\boldsymbol{\sigma}\\&\boldsymbol{Paras} = \{P_{13}, P_3, P_{45}, T_{45}, P_5, P_7\}\end{aligned} \tag{28}$$

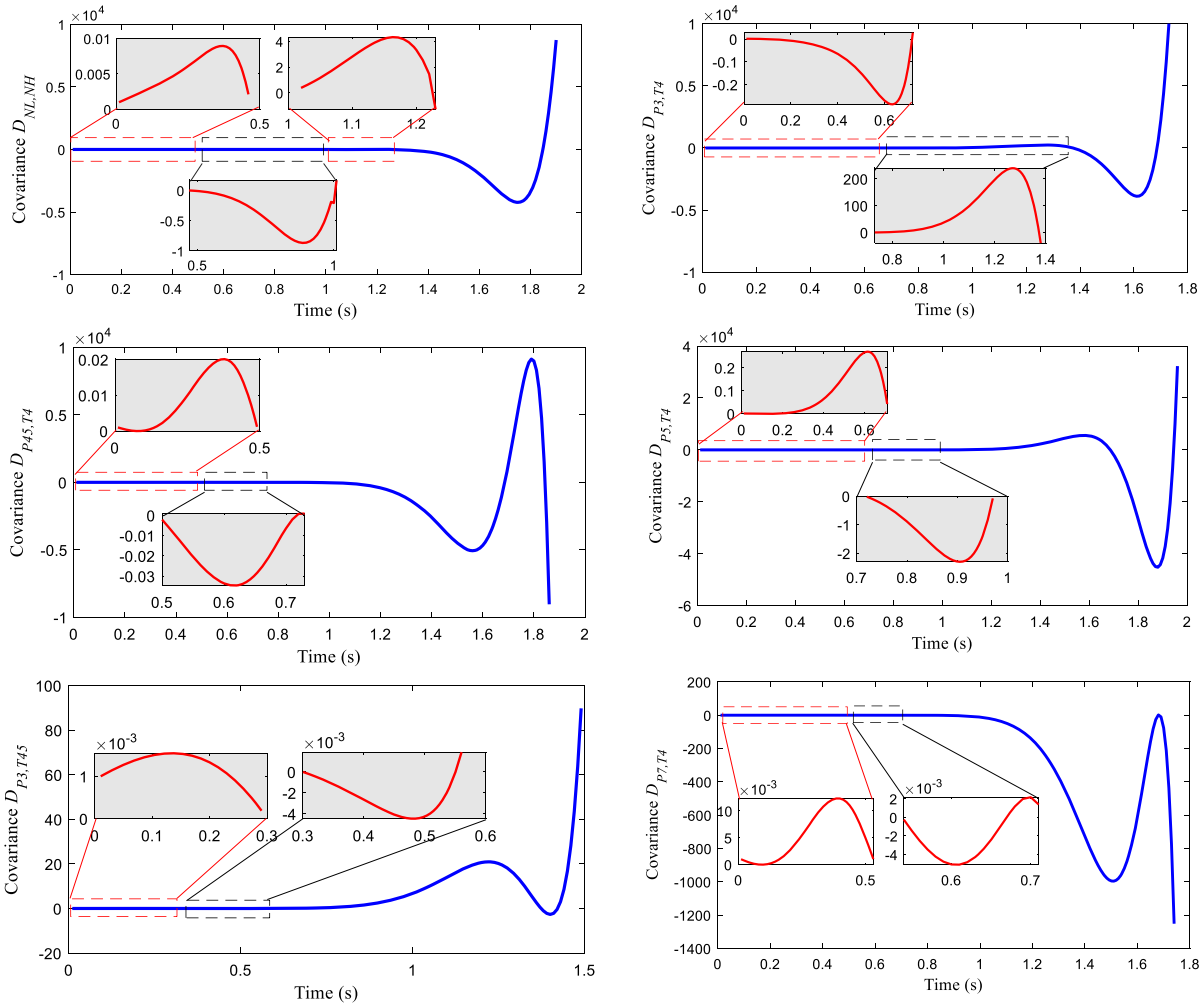

Fig. 9 Covariance evolution trends of two thermodynamic parameters under actuator uncertainties

Table 4 Parameters in the robust optimization model

Parameters	ω_1	ω_2	Lower boundary ***lb***				Upper boundary ***ub***			
			π_{total}	B_r	T_4	T_7	π_{total}	B_r	T_4	T_7
Values	0.5	0.5	32	0.25	1750	1500	42	0.45	2050	1900

where $f(\bullet)$ denotes the steady-state mechanism model of the engine system. Vector **inputs** include parameters such as altitude, Mach number, ambient temperature and pressure, fuel flow rate, speeds and so on. ω_1 and ω_2 denote the weights of thrust and SFC. The subscripts *original* and *optimized* represent the performance parameters obtained without considering the uncertainty influence and considering the uncertainty influence, respectively. ***lb*** and ***ub*** represent the optimization boundary vector of design parameters. The upper and lower boundaries of design parameters and weights are given in Table 4. Based on the variances of thermodynamic parameters shown in Fig. 4a. $\boldsymbol{Paras}_0$ represents the nominal value of thermodynamic parameters ***Paras*** under stable operation of the engine. The 3σ criterion is adopted to consider the stochastic

response distribution characteristics and further determine the ranges of ***Paras***, which are used to act as the constraints of the optimization process. σ is the standard deviation.

4.2 Performance design with robust optimization

The uncertainty will offset the performance advantages of the engine. The design process considering the influence of uncertainty aims to maximize the possibility of selecting high-quality candidate design parameters that meet the engine performance requirements, while minimizing the risk caused by uncertainty. In other words, the setting of design parameters reaches the maximum probability density of the estimated performance level in an acceptable area, while minimizing the negative impact of uncertainty factors on design performance.

In the optimization process, to avoid the stochastic impact of optimization results on the performance design, 1500 optimization experiments are performed, and the optimal design parameters are determined through the statistical analysis of optimization results. The fitness values in 1500 optimization experiments show a normal distribution, as shown in Fig. 10. When the fitness value is greater than 1, it indicates that the optimized engine performance is worse than the traditional performance design. Fitness $\in [0.9894, 0.9911]$ is the high-frequency optimization performance, and the corresponding optimization results are considered as the optimal design parameters, with a probability of 13.1%. According to Fig. 10, the optimization results of Fitness $\in [0.9894, 0.9929]$ account for 25.4% of the total experiments, and the optimization results of Fitness $\in [0.9842, 0.9998]$ account for 84.4%. The robust optimization method based on the stochastic dynamics model improves the engine performance with an approximate probability of 84.4% in the performance robust design, and the proposed robust performance optimization design method is effective and reliable.

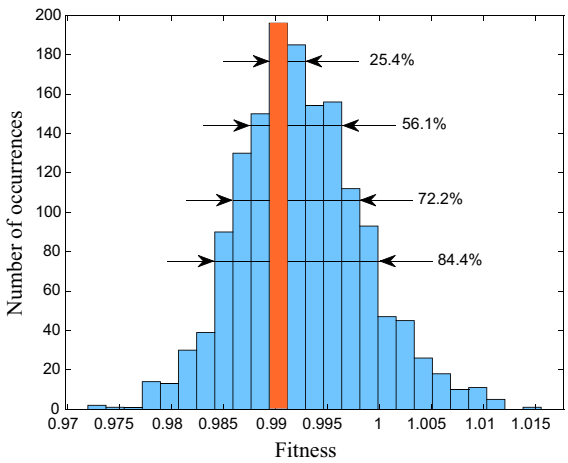

Fig. 10 Fitness distributions and probability of obtaining optimal performance in robust optimization design

Figure 11 shows the optimization results of engine design parameters obtained from 1500 optimization experiments. The total pressure ratio π_{total}, bypass ratio B_r, main combustion chamber outlet temperature T_4 and afterburner outlet temperature T_7 all show the normal distribution features, which are completely consistent with the fitness distribution form. For the total pressure ratio, bypass ratio and main combustion chamber outlet temperature, the peak probability densities are larger, indicating that the dispersions of optimization results of these three parameters are smaller and the optimal results are relatively concentrated. While the probability density of the afterburner outlet temperature is relatively small, indicating that the optimization results are relatively scattered and have great randomness. Overall, the robust optimization method obtains more concentrated optimization results and a better optimization effect. The optimization design values corresponding to the maximum probability densities are considered to be the optimal design parameters in 1500 optimization experiments. Because the maximum probability densities indicate that this group of design parameters occurs frequently in the optimization process, it is selected as the robust optimization design parameters of the engine performance. The comparisons with the design values based on the traditional mechanism model are shown in Table 5. Compared with the design results based on the traditional mechanism model without considering actuator uncertainties, the robust optimization design results based on the stochastic dynamics model improve the total pressure ratio, bypass ratio, main combustion chamber outlet temperature and afterburner outlet temperature to a certain extent, to improve the engine performance.

The thermodynamic parameters characterizing the operating states of engine components directly reflect the adverse effects of actuator uncertainties, which have obvious stochastic distribution characteristics.

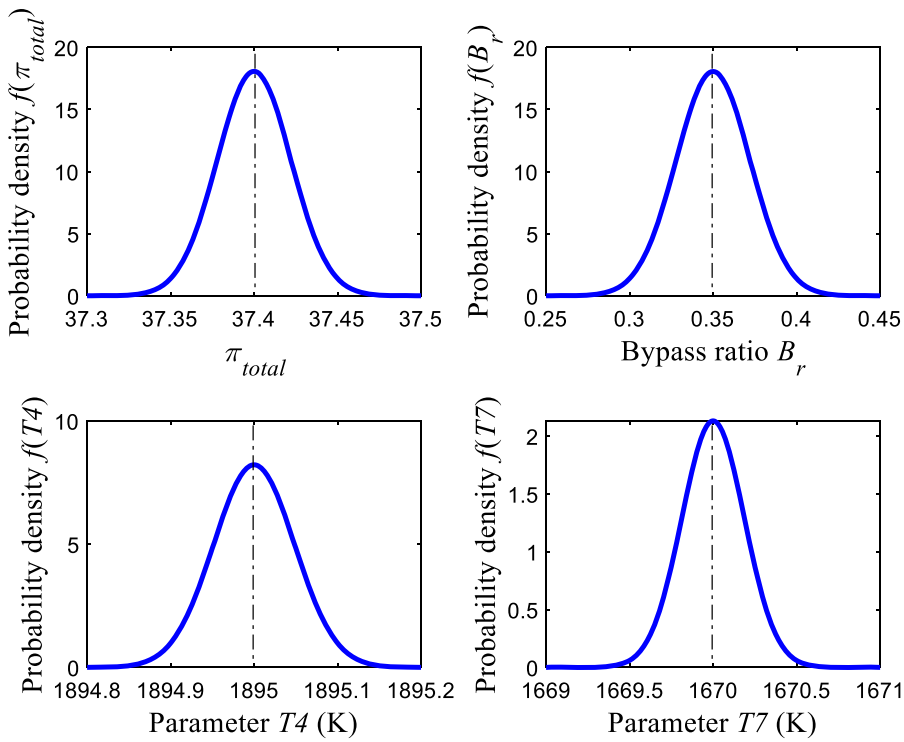

Fig. 11 Distributions of engine performance design parameters based on the robust optimization method

Table 5 Robust optimization results of engine design parameters

Methods	π_{total}	B_r	T_4	T_7
Traditional mechanism model-based design method	34.2	0.32	1873	1655
Stochastic dynamics model-based robust design method	37.4	0.35	1895	1670

These distribution characteristics act as the constraints in the robust optimization design of engine performance and limit the uncertainty influence. Their distribution characteristics in 1500 optimization experiments are shown in Fig. 12. After robust optimization, the thermodynamic parameters still show the normal distribution features, but compared with the traditional design results, the means and variances of thermodynamic parameter distributions are improved. Compared with the probability density curves obtained by the traditional mechanism model, the probability density obtained by the robust optimization method is increased by at least 0.2 and at most 0.48. The increase in the probability density shows that the design parameters obtained by the robust optimization are more concentrated and less affected by actuator uncertainties. The proposed method designs the optimal engine parameters with greater probability in the robust performance optimization design.

Figure 13 further shows the distribution characteristics of engine performance parameters. "Desired" indicates the engine thrust and SFC we expect to obtain when taking the optimization results (blue dotted line in Fig. 13) of the traditional mechanism model as a benchmark. Compared with the engine performance designed by the traditional mechanism model without considering the influences of actuator uncertainties, the engine working performance designed by the robust optimization method has been significantly improved, in which the thrust has been increased by 9.7 kN at most, and the SFC has been reduced by 0.022 kg/N/h at most. The probability density of thrust distribution has been increased by

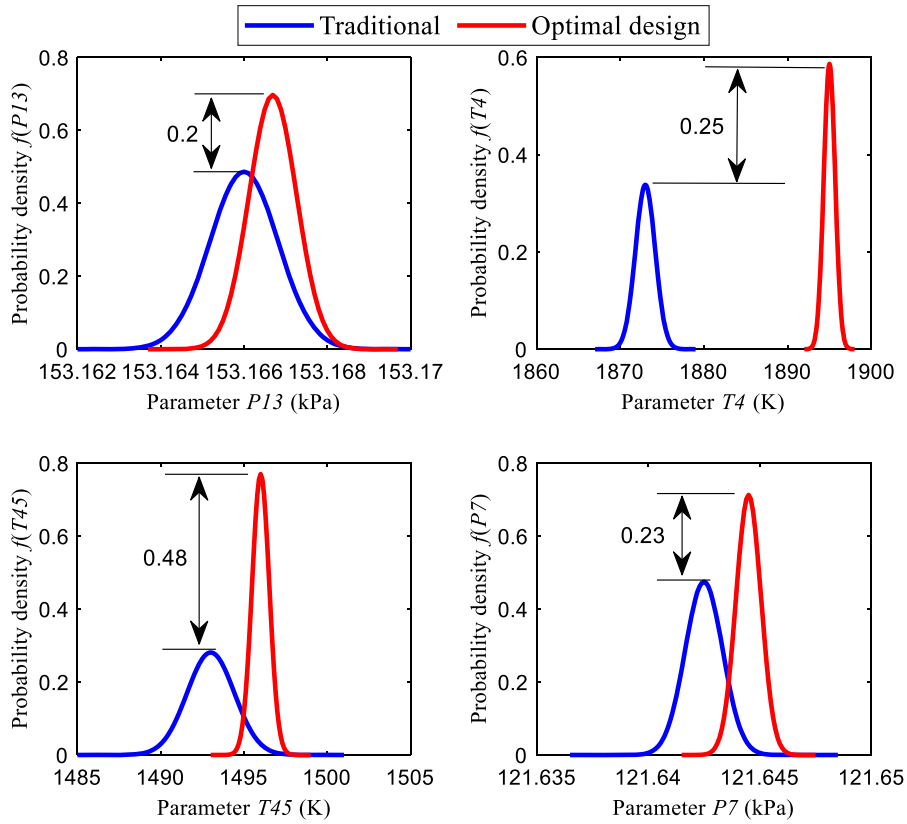

Fig. 12 Distributions of thermodynamic parameters obtained by the robust optimization method and traditional mechanism model

0.048 at most, and the probability density of SFC distribution is increased by 0.916 at most. It indicates that the engine performance distributions obtained by the robust optimization method are more aggregated; in other words, it can achieve the optimal performance design with higher probability. In addition, Fig. 13 also compares the effects of actuator uncertainties with different intensities on the engine performance. The increase in the uncertainty intensity reduces the optimal thrust and increases the SFC under the optimal design parameters, and the improvement ranges of thrust and SFC decrease. The specific comparative results are shown in Table 6.

In order to prove that the robust optimization design method is effective and reliable. The classical statistical analysis method for stochastic problems, namely Monte Carlo simulation, is used to verify the proposed method. In the Monte Carlo simulations, the ranges of design parameters are the same as those used in the robust optimization design. The engine performance is calculated by the traditional mechanism model. The performance design results of 30,000 Monte Carlo simulations are shown in Fig. 13. The distribution characteristics of performance parameters are basically consistent with the results of the robust optimization design method. Continuing to increase the number of simulation experiments will be able to obtain a higher coincidence degree, but the calculation cost is also significantly increased. On the premise that the proposed method and Monte Carlo simulation method achieve the same performance design effect, Table 7 shows the total running time when the two methods achieve the same design effect, as shown in Fig. 13. Compared with the calculation cost of the Monte Carlo simulations, the robust optimization design method saves more than half of the calculation cost and improves the relative calculation efficiency by 47.82%. Therefore, the robust optimization design method has high computational efficiency and robust performance design effect.

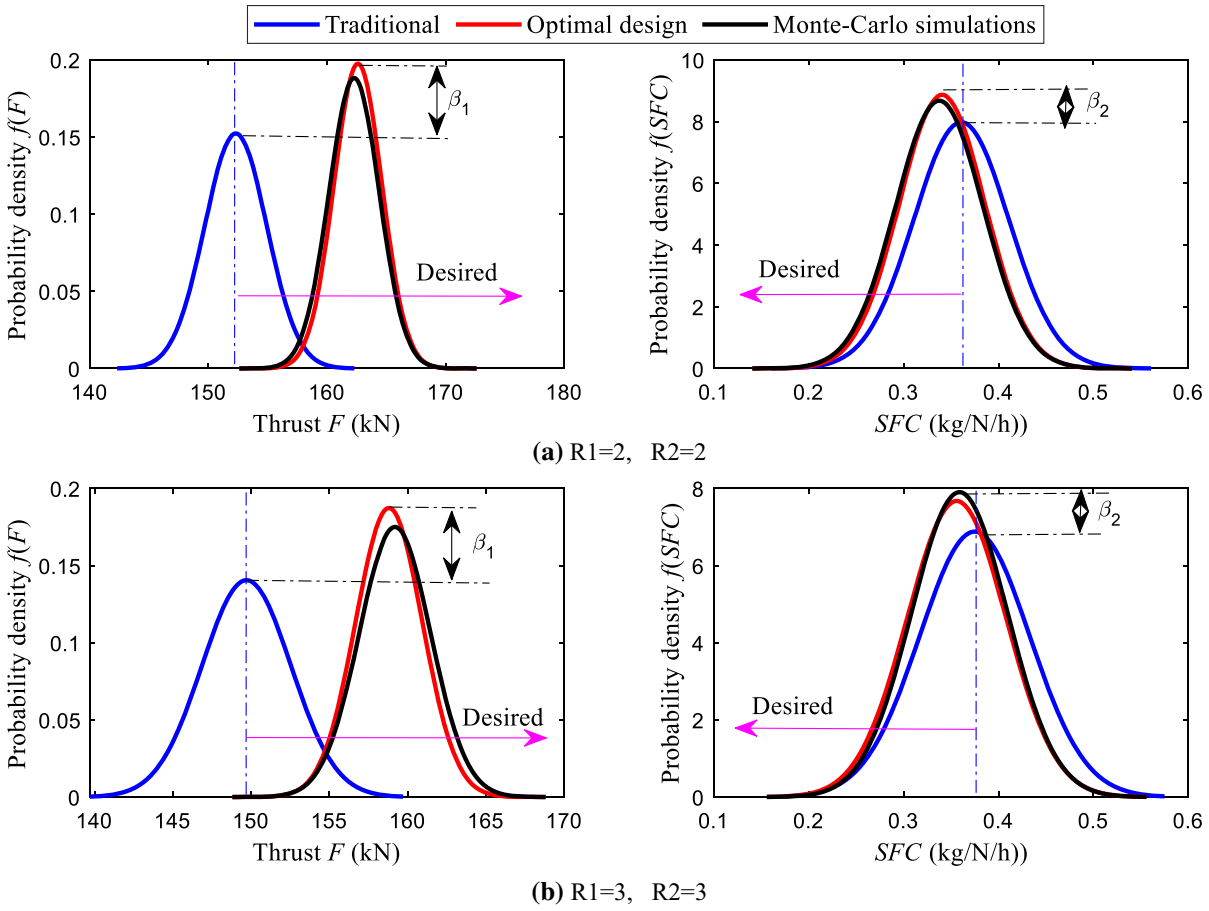

Fig. 13 Engine performance distributions under actuator uncertainties with different intensities

Table 6 Comparative results of engine performance designed by two methods

Uncertainties	δF	β_1	δSFC	β_2
R1 = 2 R2 = 2	9.7 ↑	0.048 ↑	0.022 ↓	0.916 ↑
R1 = 3 R2 = 3	8.9 ↑	0.047 ↑	0.017 ↓	0.794 ↑

5 Conclusions

A stochastic dynamics model for analyzing the influences of actuator uncertainties on engine operating states and working performance is developed based on the stochastic dynamics theory, and then, a robust optimization design method with stochastic response constraints is established for the performance design of the nonlinear engine system, which significantly reduces the uncertainty influences and improves the engine performance. The main conclusions are as follows:

Table 7 Comparisons of calculation cost in the proposed method and Monte Carlo simulations

Methods	Running time for once (s)	Number of experiments	Total running time (h)
Robust optimization design method	21.5362	1500	8.97
Monte Carlo simulations	2.0625	30,000	17.19

(1) Considering actuator uncertainties as to the external stochastic excitations of nonlinear engine system, the stochastic dynamics model is derived to realize the stochastic response characteristic analyses of thermodynamic parameters and the cooperative change trend analyses between two thermodynamic parameters. The necessity of considering the actuator uncertainties in the thermodynamic parameter analysis and performance optimization design of turbofan engines is proved.

(2) Actuator uncertainties have a great influence on the distribution characteristics of thermodynamic parameters and system performance. Compared with the nozzle actuation uncertainty, the fuel system actuation uncertainty has a greater impact on the thermodynamic parameters and system performance, which should be given priority consideration.

(3) The robust optimization method obtains the engine performance design results with lower dispersion and realizes the optimal engine performance with a higher probability. Compared with the traditional methods, the proposed method reduces the calculation cost by more than half, which has great advantages in the practical applications of performance optimization design.

(4) Compared with the traditional mechanism model without considering the uncertainty influences, the robust optimization method significantly reduces the uncertainty influences and improves engine performance.

Acknowledgements This work is supported by the Science and Technology Department of Ningxia (Grant No. 2022ZDYF1483) and Chinese-German Center for Research Promotion (Grant No. GZ1577).

Funding This work is funded by the Science and Technology Department of Ningxia (Grant No.1015 2022ZDYF1483) and Chinese-German Center for Research Promotion (Grant No. GZ1577).

Data availability The data can be provided by the corresponding author on reasonable request.

Declarations

Conflict of interest The authors declare that they have no conflict of interest concerning the publication of this manuscript.

References

1. Cheung, J., Scanlan, J., Wong, J., Forrester, J., Eres, H.: Application of value-driven design to commercial aero-engine systems. J. Aircr. **49**(3), 688–702 (2012)
2. Cao, D., Bai, G.: A study on aeroengine conceptual design considering multi-mission performance reliability. Appl. Sci. **10**(13), 4668 (2020)
3. Ding, S., Yuan, Y., Xue, N., Liu, X.: An onboard aeroengine model-tuning system. J. Aerosp. Eng. **30**(4), 04017018 (2017)
4. Xiao, L.: Aeroengine multivariable nonlinear tracking control based on uncertainty and disturbance estimator. J. Eng. Gas Turbines Power **136**(12), 121601 (2014)
5. Zhu, S.P., Huang, H.Z., Peng, W., Wang, H., Mahadevan, S.: Probabilistic physics of failure-based framework for fatigue life prediction of aircraft gas turbine discs under uncertainty. Reliab. Eng. Syst. Saf. **146**, 1–12 (2016)
6. Jin, P., Lu, F., Huang, J., Kong, X., Fan, M.: Life cycle gas path performance monitoring with control loop parameters uncertainty for aeroengine. Aerosp. Sci. Technol. **115**, 106775 (2021)
7. Dong, P., Tang, H., Chen, M., Zou, Z.: Overall performance design of paralleled heat release and compression system for hypersonic aeroengine. Appl. Energy **220**, 36–46 (2018)
8. Zhang, J., Tang, H., Chen, M.: Robust design methodologies to the adaptive cycle engine system performance: preliminary analysis. Energy Procedia **158**, 1521–1529 (2019)
9. Cai, C., Zheng, Q., Zhang, H.: A new method to improve the real-time performance of aero-engine component level model. Int. J. Turbo Jet-Engines (2020). https://doi.org/10.1515/tjeng-2020-0033
10. Wang, H., Wang, X., Dang, W., Yao, H., Wang, B.: Generic design methodology for electro-hydraulic servo actuator in aero-engine main fuel control system. Turbo Expo: Power for Land, Sea, and Air. Am. Soc. Mech. Eng. **45752**, V006T06A035 (2014)
11. Shi, Z.Y., Li, X.Z., Li, Y.K., Lin, J.C.: A high-precision form-free metrological method of aeroengine blades. Int. J. Precis. Eng. Manuf. **20**(12), 2061–2076 (2019)
12. Montazeri-Gh, M., Nasiri, M.: Hardware-in-the-loop simulation for testing of electro-hydraulic fuel control unit in a jet engine application. SIMULATION **89**(2), 225–233 (2013)
13. Montazeri-Gh, M., Nasiri, M., Rajabi, M., Jamshidfard, M.: Actuator-based hardware-in-the-loop testing of a jet engine fuel control unit in flight conditions. Simul. Model. Pract. Theory **21**(1), 65–77 (2012)
14. Dwi Atmaji, F.T., Noviyanti, A.A., Juliani, W.: Implementation of maintenance scenario for critical subsystem in aircraft engine: case study NTP CT7 engine. Int. J. Innov. Enterp. Syst. **1**(02), 52 (2017). https://doi.org/10.25124/ijies.v1i01.85
15. Satish, T.N., Murthy, R., Singh, A.K.: Analysis of uncertainties in measurement of rotor blade tip clearance in gas turbine engine under dynamic condition. Proc. Inst. Mech. Eng., Part G: J. Aerosp. Eng. **228**(5), 652–670 (2014)
16. Tao, Z., Guo, Z., Song, L., Li, J.: Uncertainty quantification of aero-thermal performance of a blade endwall considering

slot geometry deviation and mainstream fluctuation. J. Turbomach. **143**(11), 111013 (2021)
17. Zhang, M., Liu, Y., Sun, C., Wang, X., Tan, J.: Measurements error propagation and its sensitivity analysis in the aero-engine multistage rotor assembling process. Rev. Sci. Instrum. **90**(11), 115003 (2019)
18. Lu, F., Gao, T., Huang, J., Qiu, X.: A novel distributed extended Kalman filter for aircraft engine gas-path health estimation with sensor fusion uncertainty. Aerosp. Sci. Technol. **84**, 90–106 (2019)
19. Chen, M., Quan, H.L., Tang, H.: An approach for optimal measurements selection on gas turbine engine fault diagnosis. J. Eng. Gas Turbines Power **137**(7), 071203 (2015)
20. Chen, J., Ma, C., Song, D., Xu, B.: Failure prognosis of multiple uncertainty system based on Kalman filter and its application to aircraft fuel system. Adv. Mech. Eng. **8**(10), 1687814016671445 (2016)
21. Zhang, J., Tang, H., Chen, M.: Robust design of an adaptive cycle engine performance under component performance uncertainty. Aerosp. Sci. Technol. **113**, 106704 (2021)
22. Cao, D., Zhao, C., Bai, G.: DCRSM-based aeroengine cycle selection approach for multi-operating conditions performance reliability. Energy Procedia **158**, 1537–1546 (2019)
23. Kaneba, C.M., Mu, X., Li, X., Wu, X.: Event triggered control for fault tolerant control system with actuator failure and randomly occurring parameter uncertainty. Appl. Math. Comput. **415**, 126714 (2022)
24. Tang, X., Tao, G., Joshi, S.M.: Adaptive actuator failure compensation for nonlinear MIMO systems with an aircraft control application. Automatica **43**(11), 1869–1883 (2007)
25. Ariffin, A.E., Munro, N.: Robust control analysis of a gas-turbine aeroengine. IEEE Trans. Control Syst. Technol. **5**(2), 178–188 (1997)
26. Gou, L., Liu, Z., Fan, D., Zheng, H.: Aeroengine robust gain-scheduling control based on performance degradation. IEEE Access **8**, 104857–104869 (2020)
27. Liu, X., Zhang, L., Luo, C.: Model reference adaptive control for aero-engine based on system equilibrium manifold expansion model. Int. J. Control (2021). https://doi.org/10.1080/00207179.2021.2016979
28. Liu, F., Chen, M.: Robust adaptive fault-tolerant control for the turbofan aero-engine system. In: 2020 5th International Conference on Advanced Robotics and Mechatronics. IEEE, 489–494 (2020)
29. Yu, L., Sun, X.M., Gao, Y.F.: Active disturbance rejection control for uncertain nonlinear systems subject to magnitude and rate saturation: Application to aeroengine. IEEE Trans. Syst. Man Cybernet.: Syst. **52**(4), 2201–12 (2021)
30. Zhang, M., Gou, L., Jiang, Z., Sun, C.: Optimization of aero-engine H-infinity robust controller based on quantum genetic algorithm. In: 2021 12th International Conference on Mechanical and Aerospace Engineering. IEEE, 225–231 (2021)
31. Zhang, Z., Ma, X., Hua, H., Liang, X.: Nonlinear stochastic dynamics of a rub-impact rotor system with probabilistic uncertainties. Nonlinear Dyn. **102**(4), 2229–2246 (2020)
32. Profir, B.: Model validation and uncertainty qualification for the preliminary aero-engine design process. University of Southampton (2019)
33. Tong, M.T., Jones, S.M., Arcara, P.C.: A probabilistic assessment of NASA ultra-efficient engine technologies for a large subsonic transport. In: ASME Turbo Expo 2004, pp. 1–8. Austria, Vienna (2004)
34. Tong, M.T.: A probabilistic approach to aero-propulsion system assessment. Turbo Expo: Power for Land, Sea, and Air. Am. Soc. Mech. Eng. **78545**, V001T01A001 (2000)
35. Fei, C.W., Choy, Y.S., Hu, D.Y., Bai, G.C., Tang, W.Z.: Dynamic probabilistic design approach of high-pressure turbine blade-tip radial running clearance. Nonlinear Dyn. **86**(1), 205–223 (2016)
36. Ng, L.W.T., Willcox, K.E.: Monte Carlo information-reuse approach to aircraft conceptual design optimization under uncertainty. J. Aircr. **53**(2), 427–438 (2016)
37. Chen, M., Zhang, J., Tang, H.: Interval analysis of the standard of adaptive cycle engine component performance deviation. Aerosp. Sci. Technol. **81**, 179–191 (2018)
38. Fu, Q., Wang, H., Yan, X.: Evaluation of the aeroengine performance reliability based on generative adversarial networks and Weibull distribution. Proc. Inst. Mech. Eng. Part G: J. Aerosp. Eng. **233**(15), 5717–5728 (2019)
39. Zhang, J., Tang, H., Chen, M.: Linear substitute model-based uncertainty analysis of complicated non-linear energy system performance (case study of an adaptive cycle engine). Appl. Energy **249**, 87–108 (2019)
40. Zhang, Y., Jin, Y.: Stochastic dynamics of a piezoelectric energy harvester with correlated colored noises from rotational environment. Nonlinear Dyn. **98**(1), 501–515 (2019)
41. McKeand, A.M., Gorguluarslan, R.M., Choi, S.K.: A stochastic approach for performance prediction of aircraft engine components under manufacturing uncertainty. In: International Design Engineering Technical Conferences and Computers and Information in Engineering Conference. American Society of Mechanical Engineers 51739, V01BT02A045 (2018)
42. Lestoille, N., Soize, C., Funfschilling, C.: Sensitivity of train stochastic dynamics to long-term evolution of track irregularities. Veh. Syst. Dyn. **54**(5), 545–567 (2016)
43. Qiao, Z., Elhattab, A., Shu, X., He, C.: A second-order stochastic resonance method enhanced by fractional-order derivative for mechanical fault detection. Nonlinear Dyn. **106**(1), 707–723 (2021)
44. Zhang, S., Yang, J., Zhang, J., Liu, H., Hu, E.: On bearing fault diagnosis by nonlinear system resonance. Nonlinear Dyn. **98**(3), 2035–2052 (2019)
45. Qiao, Z., Liu, J., Ma, X., Liu, J.: Double stochastic resonance induced by varying potential-well depth and width. J. Franklin Inst. **358**(3), 2194–2211 (2021)
46. Shen, M., Yang, J., Sanjuán, M.A.F., Zheng, Y., Liu, H.: Adaptive denoising for strong noisy images by using positive effects of noise. Eur Phys J Plus **136**(6), 698 (2021)
47. Yang, L.P., Wang, L.Y., Wang, J.Q., Zare, A., Brown, R.J.: Nonlinear dynamics of cycle-to-cycle variations in a lean-burn natural gas engine with a non-uniform pre-mixture. Nonlinear Dyn. **104**, 1–18 (2021)
48. Yang, L.P., Bodisco, T.A., Zare, A., Marwan, N., Chu-Van, T., Brown, R.J.: Analysis of the nonlinear dynamics of inter-cycle combustion variations in an ethanol fumigation-diesel dual-fuel engine. Nonlinear Dyn. **95**(3), 2555–2574 (2019)
49. Li, S., Bastani, O.: Robust model predictive shielding for safe reinforcement learning with stochastic dynamics. In: 2020 IEEE International Conference on Robotics and Automation. IEEE, pp. 7166–7172 (2020)

50. Kühnel, L., Sommer, S., Arnaudon, A.: Differential geometry and stochastic dynamics with deep learning numerics. Appl. Math. Comput. **356**, 411–437 (2019)
51. Roberts, R.A., Eastbourn, S.M.: Modeling techniques for a computational efficient dynamic turbofan engine model. Int. J. Aerosp. Eng. (2014). https://doi.org/10.1155/2014/283479
52. Gou, L., Liu, Z., Fan, D.: Aeroengine robust gain-scheduling control based on performance degradation. IEEE Access **8**, 104857–104869 (2020)
53. Jin, P., Lu, F., Huang, J.: Life cycle gas path performance monitoring with control loop parameters uncertainty for aeroengine. Aerosp. Sci. Technol. **115**, 106775 (2021)
54. Seldner, K., Cwynar, D.S.: Procedures for generation and reduction of linear models of a turbofan engine. NASA Technical Paper 1978
55. El-Bakry, A.S., Tapia, R.A., Tsuchiya, T., Zhang, Y.: On the formulation and theory of the Newton interior-point method for nonlinear programming. J. Optim. Theory Appl. **89**(3), 507–541 (1996)